International Journal of Computational Methods
Vol. 9, No. 1 (2012) 1240013 (14 pages)

DOI: 10.1142/S0219876212400130

OVERSET-RANS COMPUTATIONS OF TWO SURFACE SHIPS MOVING IN VISCOUS FLUIDS

DECHENG WAN* and ZHIRONG SHEN

State Key Laboratory of Ocean Engineering
School of Naval Architecture, Ocean and Civil Engineering
Shanghai Jiao Tong University
Dongchuan Road 800, Shanghai, 200240, China
**dcwan@sjtu.edu.cn*

Received 14 October 2010
Accepted 4 March 2011

A structured overset grid approach coupled with Reynolds-Averaged Navier-Stokes (overset-RANS) method is presented to provide an accurate resolution of two surface ships moving with opposite velocity in viscous fluids. The RANS equations with shear stress transport (SST) $k-\omega$ model are employed to treat the viscous turbulent flows. The fully nonlinear boundary condition at the free surface is satisfied at each time step and the evolution of the free surface is achieved by using the level set method. A structured overset grid approach is used to allow flexibility in grid generation, local mesh refinement, as well as the simulation of moving objects while maintaining good grid quality. The presented overset-RANS method is demonstrated by two surface Wigley ship hulls moving with opposite velocity in still water. The simulating results illustrate the feasibility of the presented method to compute the complex viscous free surface flows interacting with many moving ships in still water or in waves.

Keywords: Dynamic overset grids; level set method; viscous flows; wave-making; multi-hull ship.

1. Introduction

A structured overset grid approach coupled with Reynolds-Averaged Navier-Stokes (RANS) method (overset-RANS) is presented to provide the accurate resolution of two surface ships moving with opposite velocity in viscous fluids. The challenge in the simulations of such viscous free surface ship flows is that the viscous effects, the free surface deformation, and the interaction of the free surface and the moving boundary of the ship hulls. Solutions of such flow problems involve the challenge of having to solve the nonlinear partial differential equations with the complexity of

*Corresponding author.

the free surface nonlinear boundary conditions and moving boundaries [Yue *et al.* (2003); Sussman *et al.* (2007); Carrica *et al.* (2004); Chang *et al.* (1996)].

In this paper, the RANS equations with shear stress transport (SST) $k-\omega$ model [Menter (1994); Carrica *et al.* (2004)] are employed to treat the viscous turbulent flows. The fully nonlinear boundary condition at the free surface is satisfied at each time step and the evolution of the free surface is achieved by using the level set method [Carrica *et al.* (2004); Sethian (1999); Paterson *et al.* (2003)]. A structured overset grid approach [Chan *et al.* (2000); Noack *et al.* (2009); Rogers *et al.* (2003)] is used to allow flexibility in grid generation, local mesh refinement, as well as the simulation of moving objects while maintaining good grid quality. A dynamic overset interpolation approach is employed to treat the moving boundary problems. The presented overset-RANS method is demonstrated by two surface Wigley ship hulls moving with opposite velocity in still water. The computed resistance coefficients, wave profiles, and wake flows for each ship hull are given, and the interacting wave pattern during the two ship hulls passing by each other are analyzed as well. The simulating results show the feasibility of the presented method to compute the complex viscous free surface flows interacting with many moving ship hulls in still water or in waves.

2. Governing Equations

The nondimensionalized RANS equations for incompressible fluid flows are as follows:

$$\frac{\partial \mathbf{u}}{\partial t} + \mathbf{u} \cdot \nabla \mathbf{u} = -\nabla p + \nabla \cdot \left(\frac{1}{\mathrm{Re}_T} \nabla \mathbf{u} \right), \quad \nabla \cdot \mathbf{u} = 0, \tag{1}$$

where $\mathbf{u}$ is velocity and p is the nondimensional piezometric pressure, which is defined by

$$p = \frac{p_a}{\rho U_0^2} + \frac{z}{Fr^2}, \tag{2}$$

where p_a is the absolute pressure, U_0 the freestream velocity, Re_T the effective Reynolds number, z the vertical distance to the free surface, and Fr is the Froude number, defined as

$$\mathrm{Re}_T = \frac{U_0 L}{\nu + \nu_t}, \quad Fr = \frac{U_0}{\sqrt{gL}}, \tag{3}$$

where L is the characteristic length, g is gravity acceleration, and ν_t is the turbulent viscosity, which is obtained by solving the blended SST $k-\omega$ model of the turbulence. Suppose that ϕ is a distance to the interface, positive in water and negative in air, then the location of the interface is given by the zero-level set of the function

ϕ, which should satisfy:

$$\frac{\partial \phi}{\partial t} + \mathbf{u} \cdot \nabla \phi = 0. \tag{4}$$

The air–water interface normal $\mathbf{n}$ and curvature κ can be computed from the level set function ϕ as follows:

$$\mathbf{n} = -\frac{\nabla \phi}{|\nabla \phi|}, \quad \kappa = \nabla \cdot \mathbf{n}. \tag{5}$$

At the interface, the interfacial boundary conditions or jump conditions apply as follows:

$$\{-p\,\mathbf{I} + \mu[\nabla \mathbf{u} + (\nabla \mathbf{u})^T]\} \cdot \mathbf{n} = -\sigma \kappa \mathbf{n}, \tag{6}$$

Where σ is surface tension coefficient. The jump conditions (6) can be integrated into Eq. (1) and the following equation can be attained:

$$\frac{\partial \mathbf{u}}{\partial t} + \mathbf{u} \cdot \nabla \mathbf{u} = -\nabla p + \nabla \cdot \left(\frac{1}{Re_T} \nabla \mathbf{u} \right) + \sigma\, \kappa\, \mathbf{n}\, \delta\,(\phi). \tag{7}$$

Since the fluid properties in Eq. (7) change discontinuously across the interface, the interface has to be smoothed across a finite thickness region that usually is a few grid points thick. Then, the fluid properties is smoothed at the interface by

$$\rho_i(\phi) = \begin{cases} 1 & \text{if } \phi > \alpha \\ \rho_i^1/\rho_i^2 & \text{if } \phi < -\alpha, \\ \bar{\rho}_i + \Delta \rho_i \sin(\pi\phi/(2\alpha)) & \text{otherwise} \end{cases} \tag{8}$$

where when $i = 1$, then ρ_1 is fluid density; when $i = 2$, then ρ_2 is viscosity coefficient; ρ_i^1 and ρ_i^2 denote two fluid properties, respectively. The α is a given interface finite thickness, $\alpha = 3/2\,\Delta x$ is often chosen in computation, here Δx is mesh size. The $\bar{\rho}_i$ and $\Delta \rho_i$ are defined by

$$\bar{\rho}_i = (\rho_i^1 + \rho_i^2)/(2\rho_i^1), \quad \Delta \rho_i = (\rho_i^1 - \rho_i^2)/(2\rho_i^1). \tag{9}$$

In Eq. (7), the following function can be applied to the $\delta(\phi)$,

$$\delta(\phi) = \begin{cases} 1/2\,(1 + \cos(\pi\phi/\alpha)) & \text{if } |\phi| < \alpha \\ 0 & \text{otherwise.} \end{cases} \tag{10}$$

3. Numerical Schemes

In order to solve the governing equations of Eqs. (7) and (4), combining a finite difference discretization and level set method is employed to compute the free surface ship flow. The steady-state solution is computed using an unsteady approach. An Euler backward difference in the time domain is applied for temporal discretization. A scheme following the PISO (pressure-implicit split-operator) [Issa (1985)]

algorithm is adopted to separate the velocity and pressure coupling. The second-order upwind biased (QUICK) scheme is used to discretize the convective terms, and the second-order central scheme is applied to the viscous term.

Besides the momentum equations and the continuity equation, the transport equation for the level set function should be also solved. From Eq. (5), the interface normal $\mathbf{n}$ and curvature κ are determined by the level set function ϕ, and the normal must be accurately evaluated at the interface because it is used in Eq. (7) and it must also be reasonable everywhere in air since it is used to extend the velocities into the air to transport the level set function ϕ. However, due to the natural consequence of the convection process in Eq. (4), the level set function ϕ may become very steep or flat in some regions, particularly in the vicinity of the interface as time goes. Therefore, for keeping ϕ as a distance function, reinitialization of ϕ is needed. We can construct a function, $\tilde{\phi}$, with the properties that its zero level is the same as ϕ and that $\tilde{\phi}$ is the signed normal distance to the interface. Here, ϕ is the level set function obtained after the level set convection step in Eq. (4), $\tilde{\phi}$ is the new level set function after reinitialization. This is achieved by solving the following problem to steady state

$$\frac{\partial \tilde{\phi}}{\partial \tau} = \text{sign}\ (\phi)\,(1 - |\nabla \tilde{\phi}|), \quad \tilde{\phi}\big|_{\tau=0} = \phi, \tag{11}$$

where sign is the sign function. From numerical purposes, the sign function can be chosen as follows:

$$\text{sign}\ (\phi) = \frac{\phi}{\sqrt{\phi^2 + \varepsilon^2}}, \tag{12}$$

where ε is a small constant. Therefore, Eq. (11) has the property that $\tilde{\phi}$ remains unchanged at the interface; therefore, the zero level set of ϕ and $\tilde{\phi}$ are the same. Away from the interface, $\tilde{\phi}$ will converge to $|\nabla \tilde{\phi}| = 1$. Therefore, it will converge to the actual distance. We can rewrite Eq. (11) in the form:

$$\frac{\partial \tilde{\phi}}{\partial \tau} + \mathbf{w} \cdot \nabla \tilde{\phi} = \text{sign}\ (\phi), \quad \mathbf{w} = \text{sign}\ (\phi) \frac{\nabla \tilde{\phi}}{|\nabla \tilde{\phi}|}. \tag{13}$$

Equation (13) has the same form as that of Eq. (4) for ϕ, and is a nonlinear hyperbolic equation whose characteristics are given by $\mathbf{w}$. The vector $\mathbf{w}$ is a unit normal always pointing outward from the zero level set ($\tilde{\phi} = 0$).

We can now summarize the above algorithm as follows:

Step 1. Initialize $\phi(\mathbf{x}, 0)$ to be signed normal distance to the free surface.

Step 2. Generate regular mesh to cover the computational domain and local mesh for each of ship, then immerse the local mesh into the background mesh. Keep the local mesh moving through the background mesh. Dynamic overset interpolation scheme is applied to exchange the data information between the background mesh and local mesh.

Step 3. Solve the Eqs. (7) and (4) for one time step with two phase fluid properties $\rho_i(\phi)$ given by Eq. (8). Denote the updated ϕ by $\phi^{(n+1/2)}$, and the updated $\mathbf{u}$, p by $\mathbf{u}^{(n+1)}$, $p^{(n+1)}$, respectively.

Step 4. Construct a new distance function $\tilde{\phi}$, and change the Eq. (11) to the following form:

$$\frac{\partial \tilde{\phi}}{\partial \tau} = \text{sign } (\phi^{(n+1/2)})(1 - |\nabla \tilde{\phi}|), \quad \phi(\mathbf{x}, 0) = \phi^{(n+1/2)}(\mathbf{x}),$$

then solve the above equation to steady state. We denote the steady-state solution by $\phi^{(n+1)}$.

Step 5. We have now advanced one time step. The zero level set of $\phi^{(n+1)}$ gives the new interface position and $\phi^{(n+1)}$ is a distance function. Repeat steps 2 and 5.

4. Numerical Experiments

Numerical simulations of two surface Wigley ship hulls moving with opposite velocity in still water are carried out to validate the presented numerical approach. Analysis will be focused on the forces in both X and Y directions, wave-profile, and free-surface in different speed and different vertical distance between two ships. The time step employed in the calculations is controlled automatically via an implicit estimation of the local truncation error of fluid velocities and pressure. In all simulations, we prescribe the geometrical and fluid quantities in dimensionless form. The Wigley hull is shown in Fig. 1. The simple geometry of this hull form is described by:

$$y = 0.5B\left(1 - \left(\frac{2x}{L}\right)^2\right)\left(1 - \left(\frac{z}{T}\right)^2\right), \tag{14}$$

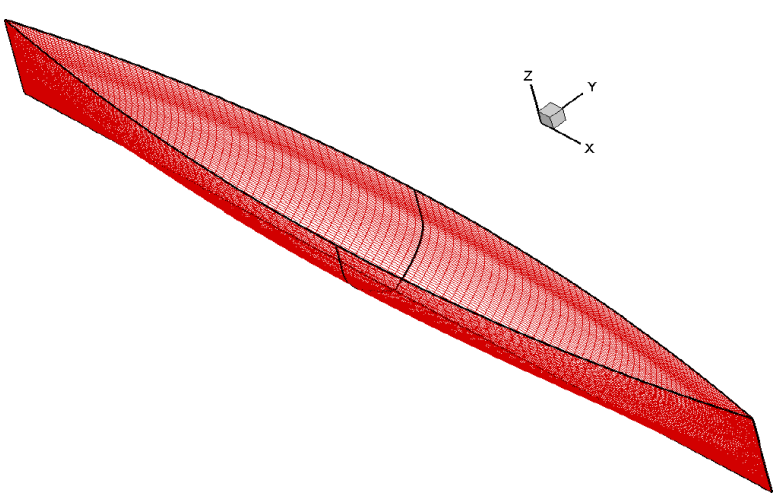

Fig. 1. The Wigley hull form.

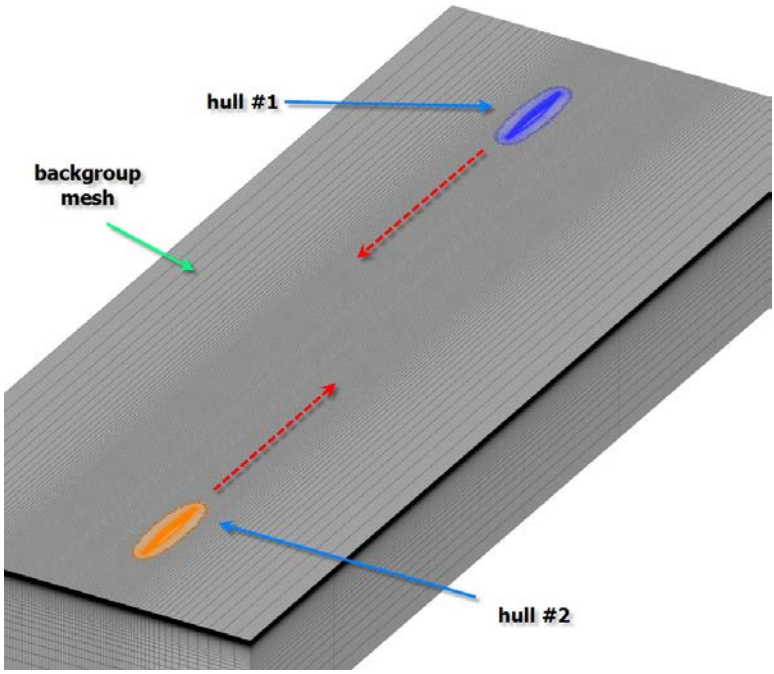

Fig. 2. Computational overset grid.

where x, y and z denote the Cartesian coordinated, hull length $L = 1.0\,\text{m}$, hull beam $B = 0.1\,\text{m}$, and ship draft $T = 0.0625\,\text{m}$.

Figure 2 presents the overset grid and the computational domain employed in the computation. The domain is 8 L in x direction, and the width and depth are set to 3.5 L and 1.5 L, respectively. Since inlet, outlet, and side boundaries are located far from the hull surface, no disturbing conditions are set on all outside boundaries. The blue mesh, which is the body fitted hull grid, is embedded into the Cartesian background grid (black grid). After hole cutting, the grid points, which reside inside the blue grid are removed, and the remaining boundary fringe points of each grid are ready to be interpolated to receive information from the other grid. And thus, the connectivity between the two independent grids is established. The initial flow is still water and the two ships are moved with specified opposite speed (Froude number Fn = 0.4). The three gaps between the two ships ($D = 1.5\,L, 1.0L$ and $0.5\,L$) are taken into account.

The computed wave patterns of two ships with different gaps ($D = 1.5\,L, 1.0\,L,$ and $0.5\,L$) passing through each other at four typical times are presented in Figs. 3–5, respectively. It can be seen that the waves are interacted more seriously when the gap between the two ships decreases.

Figure 6 shows the wave profiles at the middle gap position between the two ships, i.e., $y = 0$. The solid line represents the case of two moving ships, the dash line

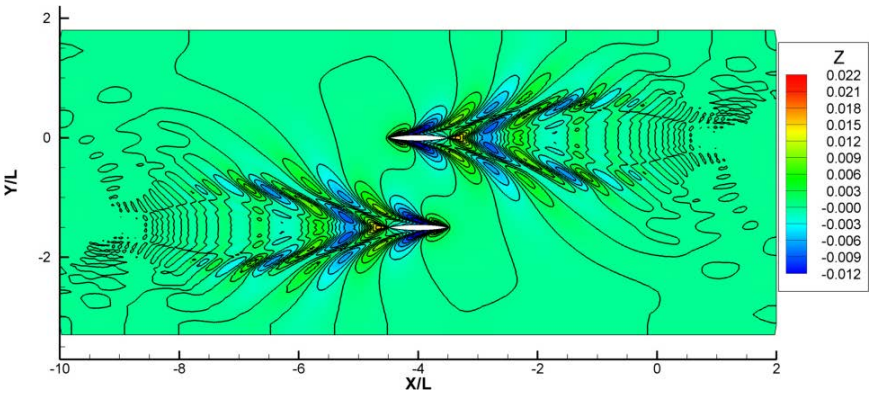

(a) $t = 5.50$

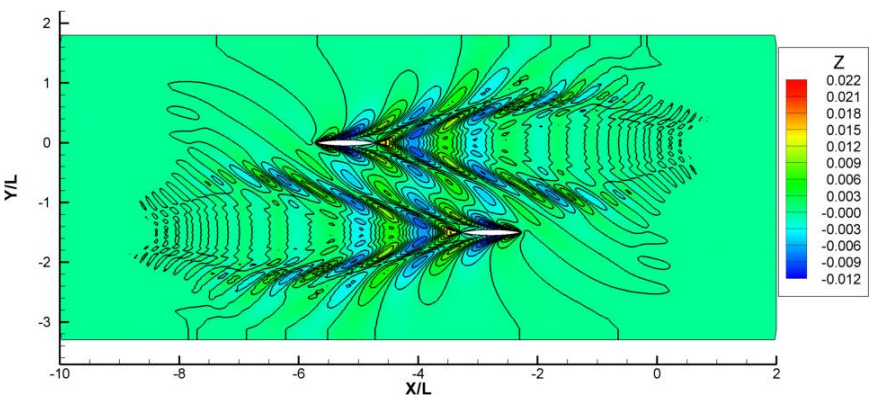

(b) $t = 6.72$

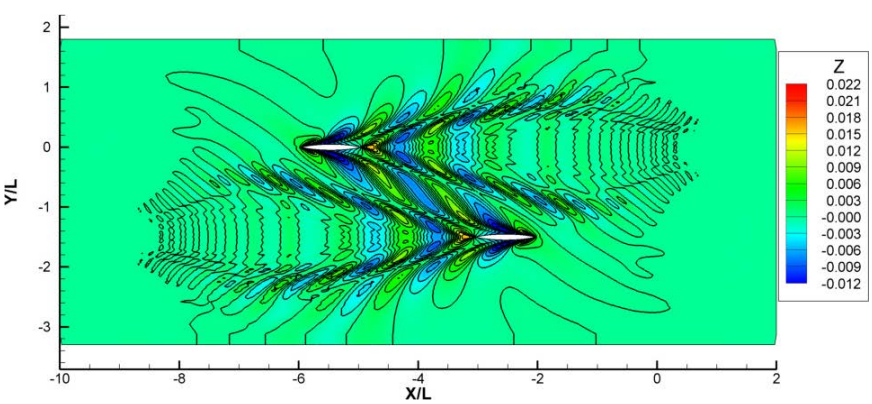

(c) $t = 6.96$

Fig. 3. Wave patterns of two ships with gaps ($D = 1.5\,L$) passing through each other.

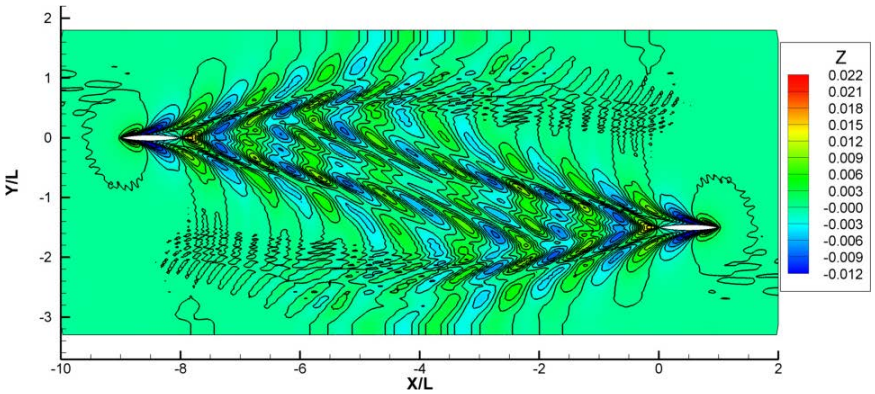

(d) $t = 10.0$

Fig. 3. (*Continued*)

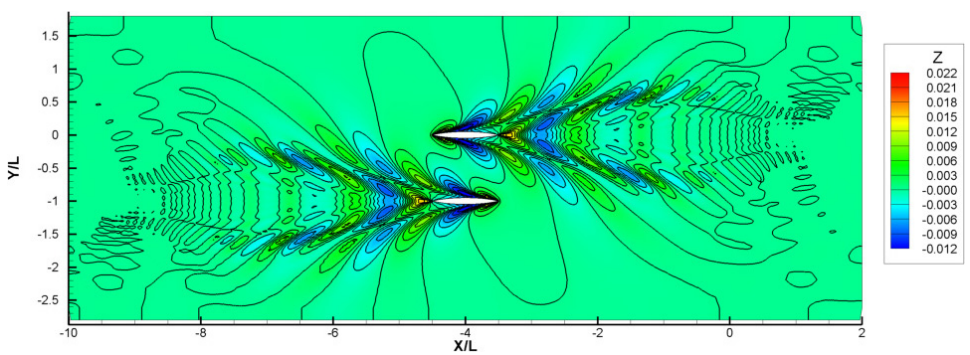

(a) $t = 5.50$

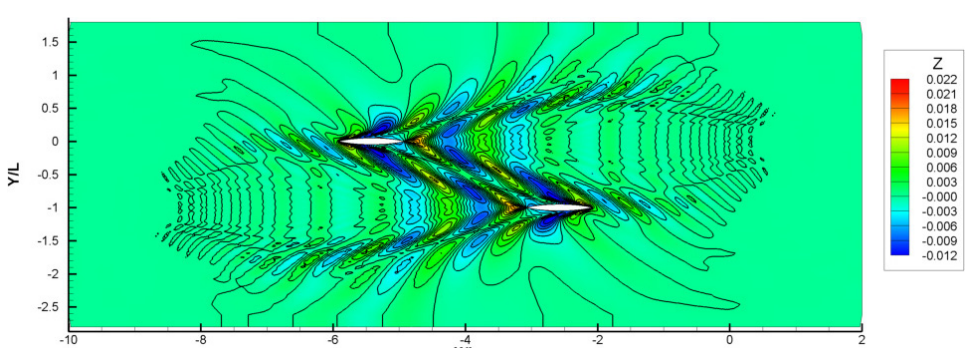

(b) $t = 6.92$

Fig. 4. Wave patterns of two ships with gaps ($D = 1.0\,L$) passing through each other.

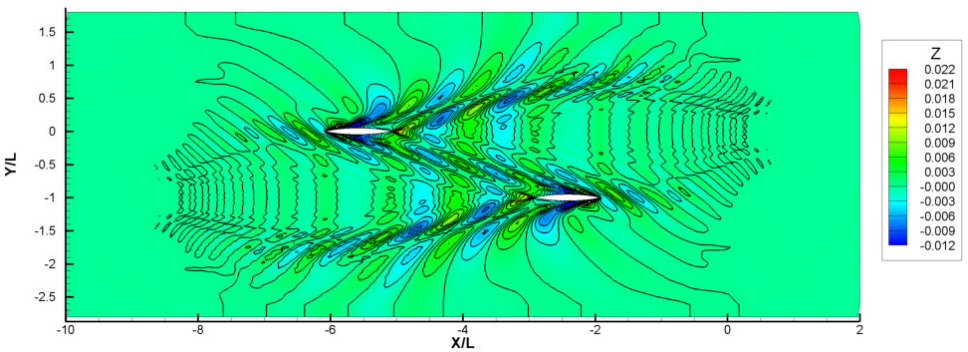

(c) $t = 7.08$

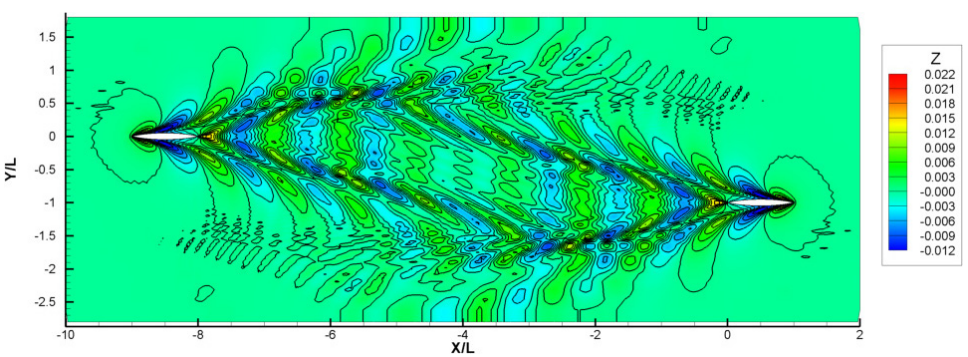

(d) $t = 10.0$

Fig. 4. (*Continued*)

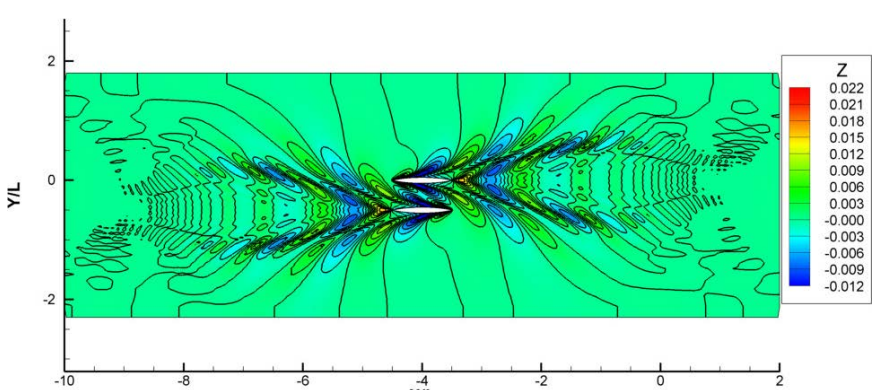

(a) $t = 5.50$

Fig. 5. Wave patterns of two ships with gaps ($D = 1.0\,L$) passing through each other.

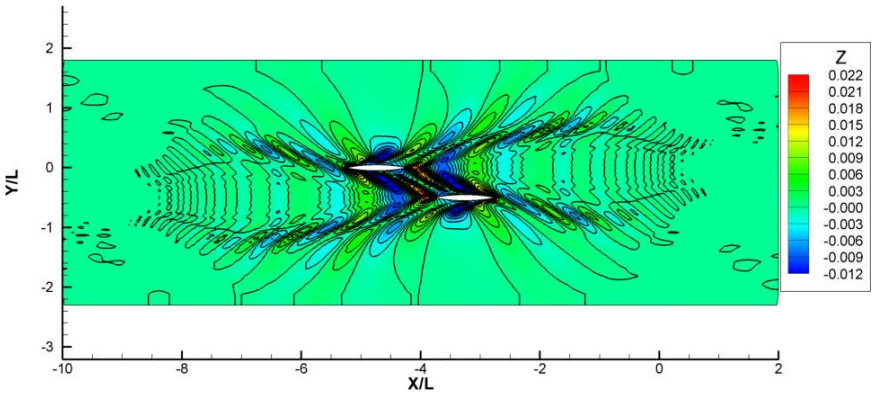

(b) $t = 6.24$

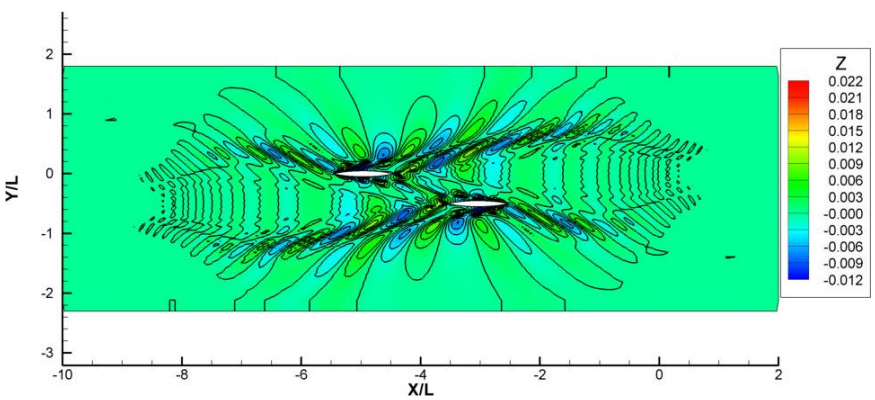

(c) $t = 6.46$

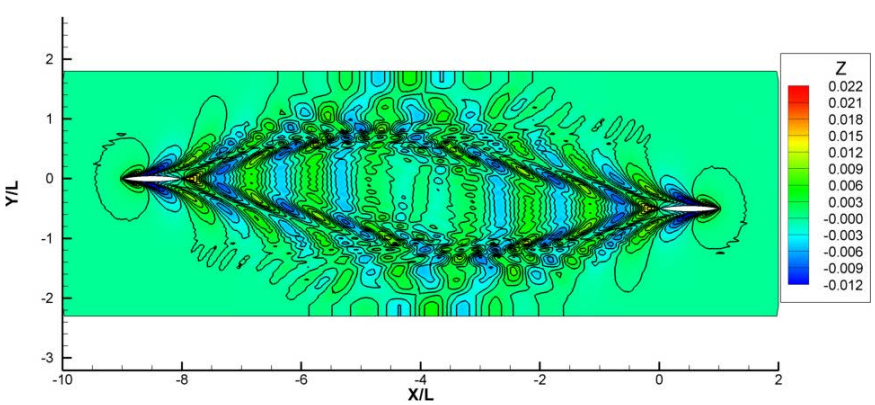

(d) $t = 10.0$

Fig. 5. (*Continued*)

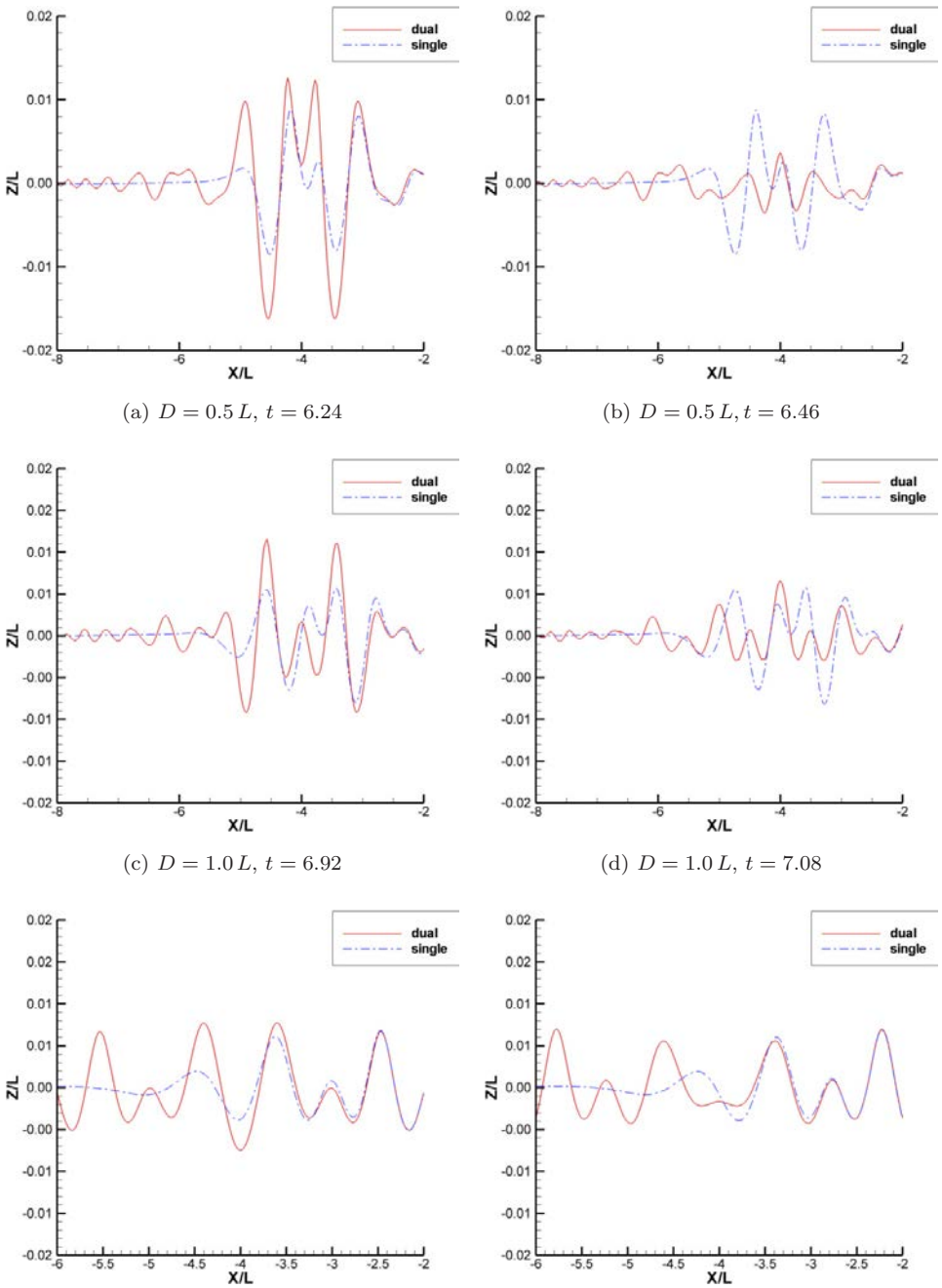

(a) $D = 0.5\,L$, $t = 6.24$ (b) $D = 0.5\,L, t = 6.46$

(c) $D = 1.0\,L$, $t = 6.92$ (d) $D = 1.0\,L$, $t = 7.08$

(e) $D = 1.5\,L$, $t = 6.96$ (f) $D = 1.5\,L$, $t = 6.72$

Fig. 6. Wave profiles at the middle gap position between the two moving ships ($y = 0$).

for the wave profiles of single moving ship but at the same position. For each gap case, two typical instances wave profiles are given. In each picture, the comparison of wave profiles between two moving ship case and single moving ship case is presented. It can be seen clearly that the surface elevation will be increased much more when the gap between the two moving ships decreased. The interaction of wave making by the two moving ships also becomes more seriously with the decrease of the two ship gap. When the two ships approach closely, the two wave-making systems start to disturb each other. The interaction of the two wave-making systems becomes serious and strong when the two ships pass through each other. Once the two ships depart far away, the wave-making system goes back to the same case of one ship-wave making system. In some instances, the wave elevation will be increased more than the single ship case; for examples, at $t = 6.24$ with gap $D = 0.5\,L$, $t = 6.92$ with gap $D = 1.0\,L$, $t = 6.96$ with gap $D = 1.5\,L$, while other instances, the wave elevation will be decreased more than the single ship case, for examples, at $t = 6.46$ with gap $D = 0.5\,L, t = 7.08$ with gap $D = 1.0\,L$, $t = 6.72$ with gap $D = 1.5\,L$. The wave profiles are changed with the motion of the two ships.

The comparison of the time history of the total resistance coefficient between two ship case with the three different gaps and one ship case is presented in Figs. 7–9, respectively. For one ship case, the resistance acting on the ship is almost a constant value; therefore, the wave-making system generated by one moving ship is steady problem. However, for the two ship case, the resistance acting on the ship is changeable, especially when the two ships pass through each other; therefore, the wave-making system generated by two moving ships is unsteady case. It can also be seen that the resistance coefficient can be changed obviously when the two ships approach and pass through each other. The changing amplitude of the resistance coefficient will be enlarged when the gap between the two ships is decreased.

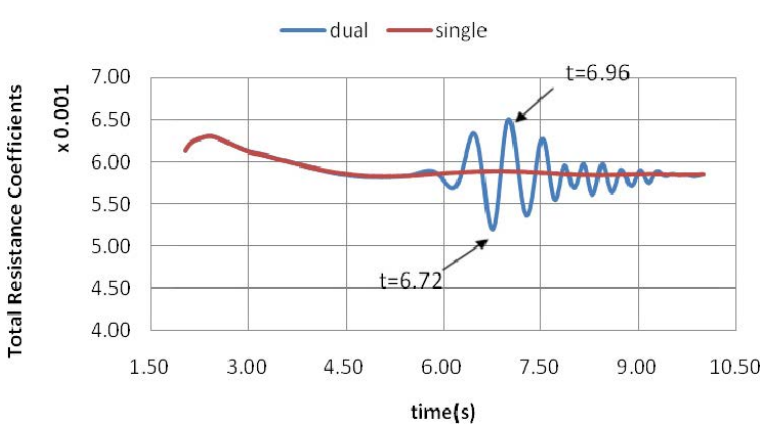

Fig. 7. The comparison of total resistance coefficient between two ship with gap $D = 1.5\,L$ and one ship case.

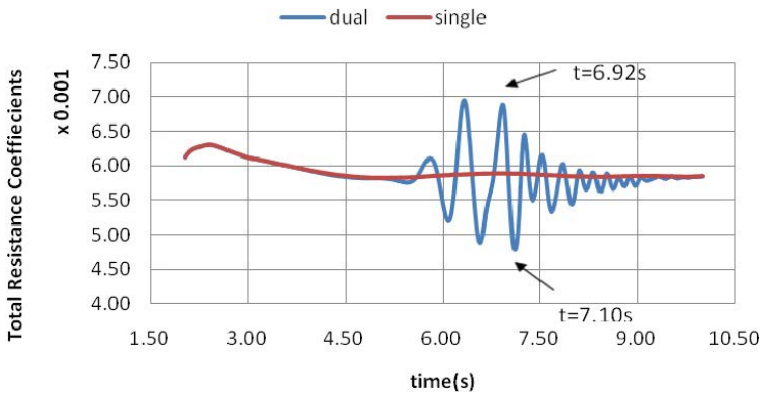

Fig. 8. The comparison of total resistance coefficient between two ship with gap $D = 1.0\,L$ and one ship case.

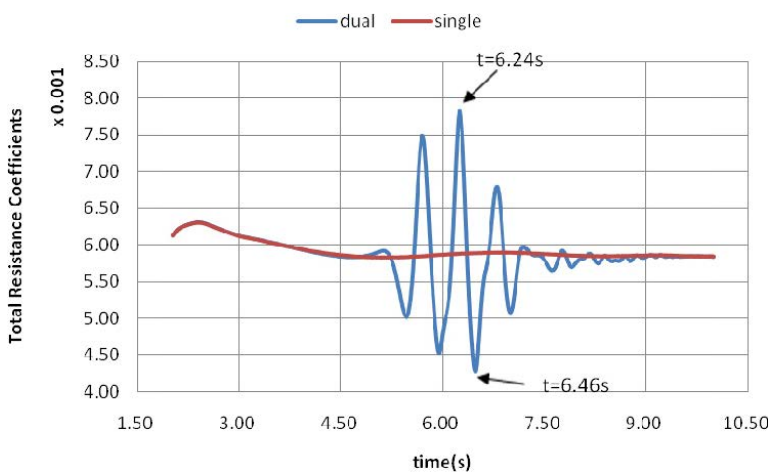

Fig. 9. The comparison of total resistance coefficient between two ship with gap $D = 0.5\,L$ and one ship case.

5. Conclusions

A combination of the 3D incompressible RANS equations with structured overset-RANS is applied to accurate resolution of two surface ships moving with opposite velocity in viscous fluids. The RANS equations with SST $k-\omega$ model are employed to treat the viscous turbulent flows. The fully nonlinear boundary condition at the free surface is satisfied at each time step and the evolution of the free surface is achieved by using the level set method. A structured overset grid approach is used to allow flexibility in grid generation, local mesh refinement, as well as the simulation of moving objects while maintaining good grid quality. The capabilities of the algorithm have been proved by two surface Wigley ship hulls moving with

opposite velocity in still water. The computed resistance coefficients, wave profiles, and wave pattern for each ship hull are given, and the interacting wave pattern during the two ship hulls passing by each other are analyzed as well. The simulating results show the feasibility of the presented method to compute the complex viscous free surface flows interacting with many moving ship hulls in still water or in waves.

Acknowledgments

The support of National Natural Science Foundation of China (Grant Nos. 50739004 and 11072154), Foundation of State Key Laboratory of Ocean Engineering of China (Grant No. GKZD 010053-11), and the Program for Professor of Special Appointment (Eastern Scholar) at Shanghai Institutions of Higher Learning for this work is gratefully acknowledged.

References

Carrica P. M., Wilson, R. V. and Stern F. [2004] Single-phase level set method for unsteady viscousfree surface flows, *Mecanica Computacional*, Bariloche, Argentina **XXIII** 1613–1631.

Chan, W. M. [2009] Overset grid technology development at NASA Ames Research Center, *Comput. Fluids* **38**(3), 496–503.

Chang, Y. C., Hou, T. Y., Merriman, B., and Osher S. [1996], A level set formulation of Eulerian interface capturing methods for incompressible fluid flows, *J. Comput. Phys.* **124**, 449–464.

Issa, R. I. [1985] Solution of the implicitly discretized fluid flow equations by operator-splitting, *J. Comp. Phys.* **62**, 40–65

Meakin, R. L. [2000] Adaptive spatial partitioning and refinement for overset structured grids, *Comput. Method Appl. Math.* **189**(4), 1077–1117.

Menter, F. R. [1994] Two-equation eddy-viscosity turbulence models for engineering applications, *AIAA J.* **32**(8), 1598–1605.

Noack, R. W., Boger, D. A., Kunz, R. F. [2009] Sugar ++: an improved general overset grid assembly capability, In *19th AIAA Computational Fluid Dynamics Conference*, San Antonio.

Paterson, E. G., Wilson, R. V. and Stern, F. [2003] General purpose parallel unsteady RANS ship hydrodynamics code: CFDSHIP-IOWA, IIHR Report No. 432, The University of Iowa.

Rhee, S. and Stern, F. [2001] Unsteady RANS method for surface ship boundary layer and wake and wave field, *Int. J. Numer. Meth. Fluids* **37**(4), 445–478.

Rogers, S. E., Suhs, N. E., Dietz, W. E. [2003] PEGASUS 5: an automated preprocessor for overset-grid computational fluid dynamics, *AIAA J.* **41**(6), 1037–1045.

Sethian, J. A. [1999] *Level Set Methods and Fast Marching Methods: Evolving Interfaces in Computational Geometry, Fluid Mechanics, Computer Vision and Materials Science*, Cambridge University Press, Cambridge.

Sussman M., Smith, K. M., Hussaini, M. Y., Ohta, M., Zhi, R. W. [2007] A sharp interface for incompressible two phase flows, *J. Comput. Phys.* **221**, 469–505.

Yue, W. S., Lin, C. L., and Patel, V. C. [2003] Numerical simulation of unsteady multidimensional free surface motions by level set method. *Int. J. Numer. Methods in Engng.* **42**, 853–884.